Audio Engineering Society

Convention Paper 10341

Presented at the 148th Convention,
2020 June 2-5, Online



# Metamaterial Absorber for Loudspeaker Enclosures

Sebastien Degraeve [1] and Jack Oclee-Brown [1]

[1] GP Acoustics (UK) Ltd.

Correspondence should be addressed to Sebastien Degraeve (sebastien.degraeve@kef.com)

**ABSTRACT**

Acoustic metamaterial absorbers can realise previously unattainable absorption spectra with sub-wavelength dimensions approaching the theoretical minimum. Such an optimal metastructure is presented in this work and implemented in a loudspeaker drive unit. The strategy is discussed and the engineering challenges are highlighted. Special attention has been paid to optimise the driver-absorber coupling and preserve the unique properties of the metamaterial absorber by using a one-parameter horn and an exact impedance match at the interfaces. The results are finally compared to exponentially tapered tubes, demonstrating the superiority of the metamaterial approach, not only in terms of performance but also versatility, size and cost.

## Introduction

Most loudspeakers are acoustic monopoles and an enclosure is used to separate the front from the rear radiation. The enclosure internal volume is related to the low-frequency extension and, as long as the wavelength is much longer than the enclosure dimensions, the box acts as a pure compliance [1]. However, at higher frequencies acoustical cavity-resonances occur and these may lead to frequency response aberrations as a result of irregularities in the loading impedance experienced by the driver. Acoustical wadding is commonly added to the enclosure to reduce the amplitude of the cavity resonances. The wadding quantity must be sufficient to prevent any aberrations in the frequency response but an excess is not desirable either as the low-frequency bandwidth is reduced [2].

In multi-way loudspeakers, some of the drivers are typically only used in the upper part of their bandwidth and the ideal enclosure behaviour is solely guided by the lack of sound colouration. A particularly useful way to look at the acoustics is to consider the reflection of the rear sound by the enclosure. The ideal situation would be zero acoustic reflection, leading to the best possible sound quality with the enclosure behaviour fully controlled.

A number of manufacturers have attempted to reach this ideal by arranging a wide open duct directly behind the diaphragm to allow the rear sound to propagate away with a minimum back reflection. In 1967 KEF used an 80 cm - long damped pipe to load the midrange unit of the Carlton speaker to encourage a progressive attenuation over the length (see Figure 1). The solution relies essentially on the fibrous or porous material properties, which are inherently inconsistent, inefficient at low frequencies and exposed to frame resonances [3].

A more effective but expensive option is to optimise the impedance match between the driver and the acoustic load. In 1940 Terman [4] patented a sound-absorbing apparatus that absorbs the backside radiation from a loudspeaker using a horn. As depicted in Figure 2, the principle is to continuously adapt the impedance from the back of the driver to the end of the cabinet in order to prevent any reflection. Despite its effectiveness, better than a simple pipe as used in the KEF Carlton, this technology suffers from several drawbacks in addition to the cost and a limited control of the wadding acoustical properties. The most obvious is the size: to work correctly, horns should be very long. Indeed, a truncated horn introduces ripples in the frequency response due to

finite-length resonances. Ripples can be reduced by using damping materials but the rise of the acoustic impedance annihilates the benefits of using a horn. There is thus a trade-off between performance and practical size. What was not a problem in 1940 is not acceptable nowadays when market requirement tends to miniaturisation.

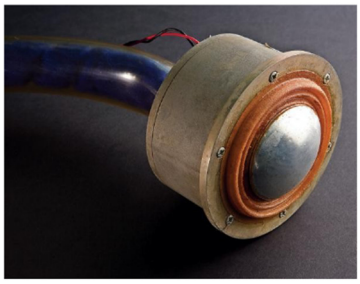

Figure 1 – KEF Carlton type 6432 midrange driver from 1967 with a resistive tube rear loading.

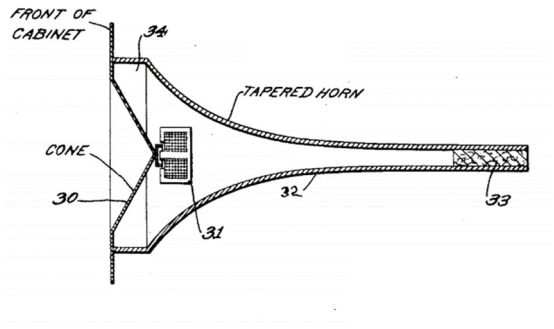


Figure 2 – F. E. Terman, "Sound Absorbing Apparatus". Patent US2293181A, 17 July 1940, using a reverse tapered horn to minimise rear reflection.

To shrink the size of the rear absorber, one possible approach is to use resonant acoustical absorbers such as Helmholtz oscillators or quarter-wavelength ducts. Acoustical resonators are extremely efficient sub-wavelength absorbers but they have the disadvantage of being narrowband in character. Adding damping increases the bandwidth but limits the absorption. An ideal solution would be to arrange a structure containing many high-Q resonators optimised to provide a wide bandwidth of overall absorption. In this context, acoustic metamaterials can deliver unconventional effective properties without the constraints normally imposed by nature. The success of the presentation of some potential applications of these extremely innovative technologies at the New York AES Convention last year [5], in front of a large audience, indicates the growing interest regarding acoustic metamaterials in the audio industry. With a metamaterial the required macro-properties are synthesised by creating a highly customised miniaturised structure. Typically, but not exclusively, a small unit-cell structure is repeated to create a larger region of material having highly optimised properties. Metamaterials now exist for many applications not restricted to acoustics and, during the past decade, acoustic metastructures have demonstrated levels of performance far exceeding the limits of conventional sound-absorbing structures [6]. A particularly optimal design of a broadband acoustic absorber developed in 2017 by Yang *et al.* [7] is briefly described in the next section.

## Causal-optimal acoustic absorbers

The concept of causal-optimal absorbers was originally proposed for electromagnetic waves [8] [9] and then adapted to room acoustics by Yang *et al.* They derive an expression linking the target absorption spectrum with the theoretical minimum thickness of a flat absorbing material sitting on a reflecting substrate. Subsequently they propose a conceptual metamaterial absorber with a theoretical minimum thickness approximately $1/10^{\text{th}}$ a wavelength of the lowest frequency to be absorbed. The absorber contains a continuum of acoustical resonators, tuned to have a constant number of resonances per octave above a cut-off frequency $f_c$. The acoustical impedance of such a metamaterial is

$$\frac{Z_{meta}}{Z_0} = \frac{\pi}{\pi + 2j\tanh^{-1}(f_c/f)} \qquad (1)$$

where $Z_{meta}$ denotes the acoustical surface impedance, $Z_0$ is the characteristic impedance at the aperture and $f$ is the frequency.

Figure 3 shows the behaviour of the real and imaginary parts of $Z_{meta}/Z_0$ normalised to $f_c$. The real part rises immediately beyond $f_c$ and

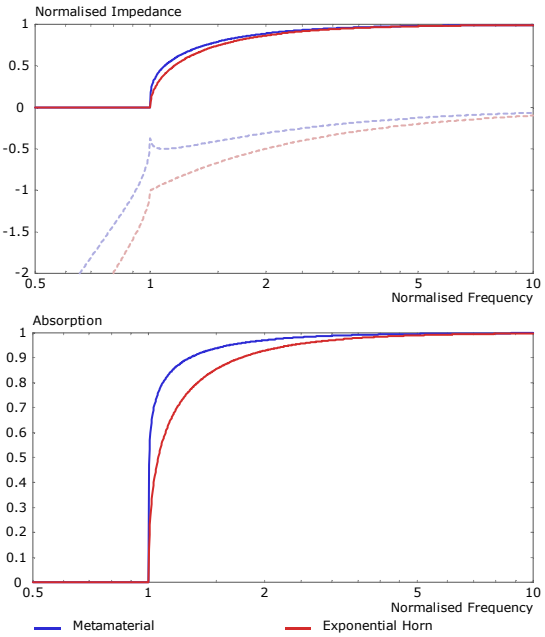


Figure 3 – Comparison of the normalised input impedance (real: solid lines, imaginary: dashed lines) and the absorption spectrum between a causal-optimal metamaterial absorber and an infinitely long exponential horn showing that a metamaterial is a more effective absorber than an infinite horn.

asymptotically approaches unity as frequency increases. The imaginary part is proportional to $(jf)^{-1}$ above $f_c$, showing that the metamaterial absorber behaves like a compliance. Below $f_c$ and as expected, the metamaterial is just a pure compliance related to the physical volume of the system. The absorption coefficient $A$ is also plotted and deduced from

$$A = 1 - \left| \frac{Z_{meta}/Z_0 - 1}{Z_{meta}/Z_0 + 1} \right|^2 . \qquad (2)$$

It can be seen that the metamaterial absorber acts as a high-pass filter and achieves almost perfect absorption above $f_c$ even if there is infinitesimal dissipation in each resonator. The behaviour of an infinitely-long exponential horn is shown for comparison and the same ideal load is achieved in the short-wavelength limit. Indeed Hanna *et al.* [10] demonstrated in 1924 that a horn has a minimum reflection when its area expansion is exponential. The results clearly show that, for the same cut-off frequency, a metamaterial is a more effective absorber than a horn, even if the latter is infinitely long. Repeating the comparison with the normalised physical volume instead of the cut-off frequency yields the same result. A horn does not provide much freedom to optimise the absorption spectrum, in contrast a metamaterial can be highly customised. The horn absorption was computed with the following coefficient of reflection:

$$R_{exp} = \frac{j\omega - \left( \frac{mc}{2} + \sqrt{\left(\frac{mc}{2}\right)^2 - \omega^2} \right)}{j\omega + \left( \frac{mc}{2} + \sqrt{\left(\frac{mc}{2}\right)^2 - \omega^2} \right)} \qquad (3)$$

where $\omega \equiv 2\pi f$ is the angular frequency, $c$ is the speed of sound and $m = 4\pi f_c / c$ is the area expansion rate.

## Metamaterial unit

The metamaterial unit described above is a multi-resonator system whose size and resonance density are optimised. In their original work, Yang *et al.* demonstrated the performance of a metamaterial absorber with 16 closed channels optimally packed into a unit cell. The metamaterial resonances are provided by both the fundamental resonance and also the harmonics of each channel. Figure 4 shows that the channels are folded to be as close as possible to the minimum theoretical thickness.

Since the resonators are very high Q, the absorption approaches 100% close to the resonance frequencies. However, the absorption drops to 50-80% at the antiresonances because the spectral density is very low. An absorbing material (sponge) is added in front of the metamaterial to create an "absorption valley-filling" effect due to the surface impedance renormalisation by the evanescent waves, and their interaction with a highly dissipative medium. It should be noted that this flat absorption feature cannot be obtained without the predesigned mode density.

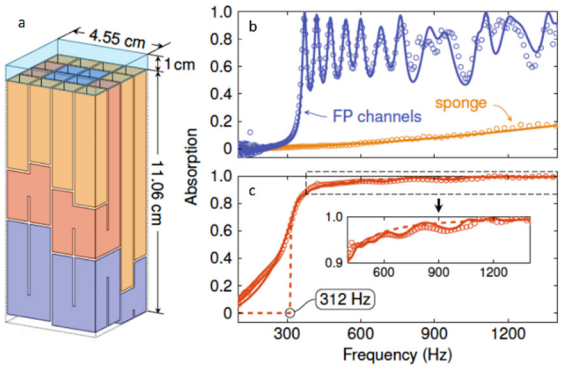


Figure 4 – a: Original metamaterial unit described in [7] consisting of 16 resonant channels with $f_c$=312 Hz. b shows separately the absorption coefficient of the metamaterial absorber and the 1 cm sponge whereas c shows the overall absorption of the hybrid solution. Solid lines are the simulation results and the circles are the experiment results obtained with a plane-wave tube.

## Application in a loudspeaker enclosure

A metamaterial loudspeaker enclosure was developed for a tweeter using the arrangement described by Yang *et al.* This work was a collaboration between KEF R&D and Acoustic Metamaterials Group (AMG), with AMG providing the design and geometry of the metamaterial structures. The metamaterial depicted in Figure 4 is not particularly well suited for a tweeter driver, which normally has a circular geometry. Figure 5 shows two potential locations where the metamaterial could be incorporated into the tweeter, either by having an axial or a radial arrangement. Figure 6 shows two metamaterial structures designed for these two locations.

The axial arrangement places the metamaterial directly behind the diaphragm. The benefit of this approach is that the acoustical behaviour of the enclosure can be almost entirely dictated by the metamaterial. However, the space directly behind the diaphragm is limited by the presence of the loudspeaker motor system. This makes the design and manufacture of the metamaterial much more challenging due to practical limitations on minimum wall thickness. In particular, since the structural walls of the metamaterial occupy volume, this space restriction severely limits the effective open area that the metamaterial presents to the rear sound and consequently the path of the rear sound wave is significantly impeded. This issue is particularly severe if, in order to increase the viscous losses, extremely narrow metamaterial channels are used resulting in more walls.

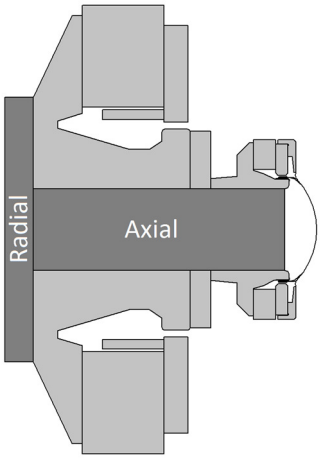


Figure 5 – Cross-section of a coaxial driver showing two potential absorber locations, one to suit an axial channel arrangement and the other a radial channel arrangement.

A radial metamaterial is a more versatile arrangement. The rear sound is channelled from the diaphragm to the metamaterial through a large area and low impedance duct with minimal or no porous acoustic wadding. This arrangement is very effective at allowing the majority of the rear sound to propagate to the metamaterial absorber which can be located further away from the diaphragm into an area where space is available. This allows much more freedom over the metamaterial design, mechanical construction and design for manufacture, such as flat injection tools. This arrangement is therefore a better choice.

Figure 7 represents the pressure spectrum of the radial absorber depicted in Figure 6, taken at the closed ends of the 30 channels, while Figure 8 shows the pressure distribution in the first resonator at 620 Hz. The first resonance $f_1$=620 Hz fixes the cut-off frequency of the absorber $f_c$ and the flat absorption spectrum is then achieved by having an equally spaced resonance

distribution per octave. Above the frequency of the first harmonics $3f_1$=1860 Hz, the new fundamental resonances complement the existing harmonics to keep the same spectral density and so on, explaining why the distribution appears less regular.

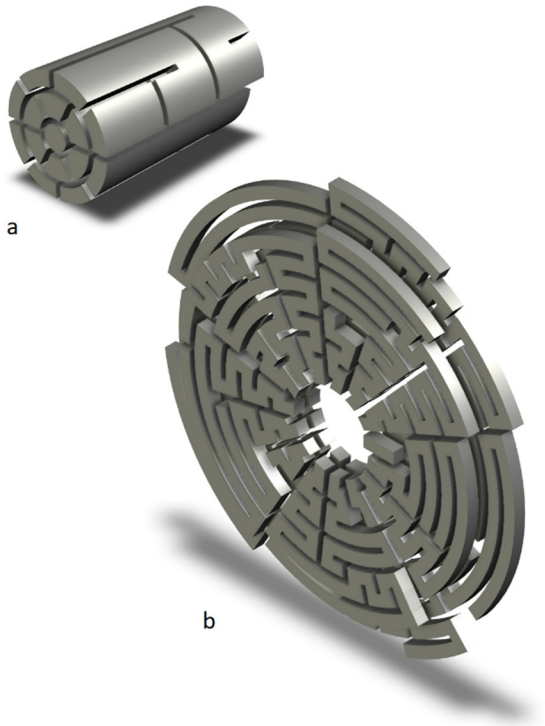


Figure 6 – Fluid path of the metamaterial absorber: axial (a) vs radial (b) arrangement.

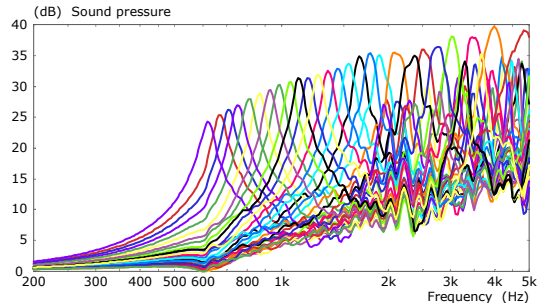


Figure 7 – Pressure level response at the closed end of each channel of the radial absorber, depicted in Figure 6 computed by finite element analysis.

Figure 8 – Pressure distribution computed by finite element analysis for the first resonance at 620 Hz, showing that only one channel is excited. The second layer is in the background, explaining why the rendering of the channels geometry is sometimes altered.

The obvious conclusion with this reasoning is that the more the number of resonators, the smoothest the response. However, keeping the same total surface area at the entrance, a large number of tubes means they become thinner and the thermosviscous losses increase the impedance of the absorber and the absorption drops as can be seen in Figure 9 when 500 tubes are used.

When using only 15 tubes, an equivalent performance to the original metamaterial unit described in [7] is achieved. The resonances are able to locally approach 100% absorption but the spectrum is not smooth. Adding a piece of absorbing material in front helps, however, since the specific acoustic impedance of wadding materials is higher than air, this leads to a non-optimal design with a higher reflection coefficient and an increased acoustical load impedance, resulting in higher back pressure behind the diaphragm. A lumped-element model of the multi-resonator metamaterial absorber has been developed and validated against the finite element analysis results; it allows us to explore the trade-offs very quickly and 30 tubes appears to be the best compromise for this specific application.

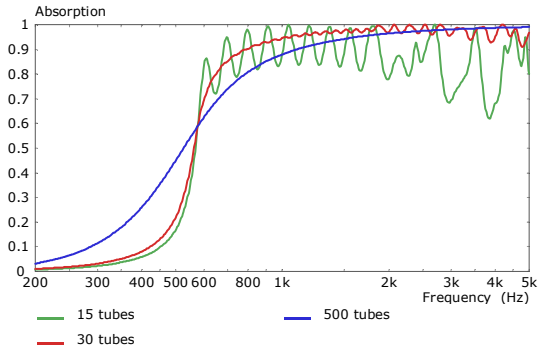


Figure 9 – Influence of the number of tubes on the absorption, the total entrance surface area being the same. 30 tubes is a good trade-off between absorption and smoothness.

A dedicated impedance tube was built to assess the performance of the actual extremely compact absorber depicted in Figure 10. The impedance tube inner diameter matches the absorber entrance diameter (14 mm) and the two ¼" microphone spacing is 30 mm, allowing accurate measurement of the coefficient of reflection between 500 Hz and 5 kHz [11]. This is indeed the region of interest because the transition slope as well as the plateau value are covered.

Figure 10 – Metamaterial absorber made with two injection molded parts. The overall thickness is only 11 mm.

The results are presented in Figure 11, demonstrating an excellent agreement between the theory and the measurement. The deviation at low frequency is related to the inaccuracy of the measurement between the two microphones as the distance is small compared to the wavelength whereas the small discrepancies between 1.5 and 3 kHz are related to the leakage between the channels. Indeed, controlling the flatness of the injection moulded parts is challenging and this issue is being resolved as this article is written. The overall performance is nevertheless extremely acceptable with an average absorption of 95%, especially considering that the tubes are empty. Fine tuning can still be achieved by using a small amount of absorbing material strategically located in front of the absorber, as it will be shown later.

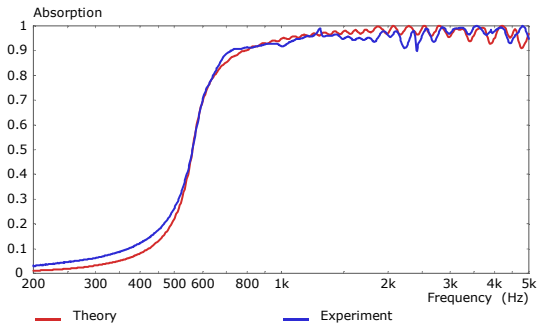


Figure 11 – Theoretical absorption of the 30-tube metamaterial absorber, computed using a lumped-element model, compared to the impedance tube experiment.

## Optimal driver-absorber coupling

In most drivers space directly behind the diaphragm is occupied by motor system parts, therefore the near-perfect broadband absorber described in the previous section should be coupled to the diaphragm through a waveguide. A variety of waveguides exists but a condition to preserve the unique properties of the metamaterial absorber is to use a one-parameter horn; meaning waves are not diffracted during the propagation, hence the coefficient of reflection is exactly zero in the waveguide itself. A straight tube, as depicted in Figure 5, is one of these non-dispersive guides. A second consideration is that the impedance

should match at the interface between the waveguide and the absorber.

The three unique one-parameter horns are the tube, the cylindrical guide and the conical horn: they can respectively carry plane, cylindrical or spherical waves without affecting their front shape [10]. The tube is discarded because its load is purely real and the impedance of the absorber is complex (see Figure 3). The cylindrical guide is not very practical and does not fit in the driver design very well, furthermore it can be easily demonstrated that it is not possible to have a good impedance match with the absorber. The remaining waveguide is the conical horn whose normalised throat impedance is

$$\frac{Z_{conical}}{Z_0} = \frac{(kr)^2 + jkr}{1 + (kr)^2} \tag{4}$$

where $k \equiv 2\pi f/c$ is the wavenumber and the radius $r$ is the distance between the throat, which is a spherical cap, and the apex [12]. Recalling that the metamaterial absorber behaves like a compliance, a minimum requirement for the waveguide is to have a negative imaginary part. The sign is positive in Eq. (4) because horns are traditionally used to expand waves and the entrance is located at the throat. This inertance term is also naturally part of the radiation impedance of the freely propagating spherical wave.

The conjugate of Eq. (4),

$$\frac{Z_{conical}}{Z_0} = \frac{(kr)^2 - jkr}{1 + (kr)^2}, \tag{5}$$

solves the problem and indicates that the horn is used in reverse and driven from the mouth. The negative imaginary part exhibits a contraction of the wavefront while propagating, resulting in a compliant behaviour, exactly like the metamaterial absorber, which is closed.

The comparison of the impedances (1) and (5) is performed in the useful bandwidth, *i.e.* above $f_c$. Using Laurent series expansion, the high-frequency behaviour of the metamaterial absorber impedance is deduced:

$$\lim_{f\to\infty} \frac{Z_{meta}}{Z_0} = 1 - \left(\frac{2f_c}{\pi f}\right)^2 - j\frac{2f_c}{\pi f} + O(f^{-3}) \tag{6}$$

In the same manner, the high-frequency impedance of the conical horn is

$$\lim_{f\to\infty} \frac{Z_{conical}}{Z_0} = 1 - \left(\frac{c}{2\pi f r}\right)^2 - j\frac{c}{2\pi f r} + O(f^{-3}) \tag{7}$$

The identification term by term of the Eqs.(6) and (7) shows that both the expression of the real and imaginary parts are similar when the distance between the throat and the apex is equal to a quarter of a wavelength of the cut-on frequency:

$$r = \frac{\lambda_c}{4} = \frac{c}{4f_c}. \tag{8}$$

The interpretation of this result is graphically depicted in Figure 12 and Figure 13, showing that the driver-absorber coupling is optimal when $r = \lambda_c/4$. The two conditions initially exposed at the beginning of the paragraph are thus fulfilled using a one-parameter horn that has an exact impedance match at the interface. Note that this is only valid at high frequencies and this restricts the length of the duct. Indeed, according to Figure 13 and as a rule of thumb, the first longitudinal resonance frequency of the duct should exceed $3f_c$ to avoid any irregularities in the frequency response.

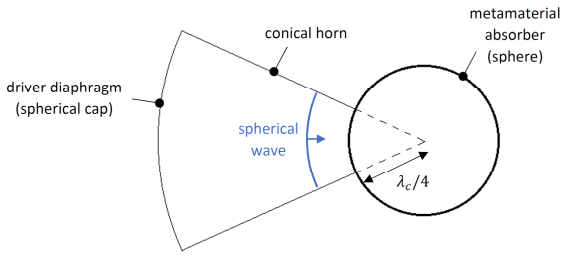


Figure 12 – A spherical wave travelling along a conical horn is almost not reflected at the horn/absorber interface if the interface radius is equal to a quarter of a wavelength of the metamaterial cut-on frequency.

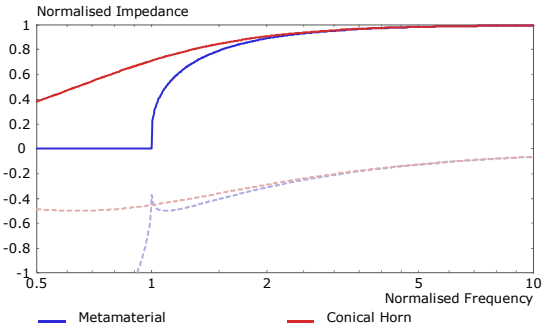


Figure 13 – Comparison between the metamaterial absorber impedance and the horn impedance when the condition (8) is satisfied: there is an almost perfect impedance match above $3f_c$. (real: solid lines, imaginary: dashed lines).

A conical horn exhibits therefore a clear advantage compared to a straight pipe in terms of reflections but, additionally, a tapered duct is also very practical for a number of reasons:

- Commonly dome-shaped diaphragms are used on high-frequency units and the concave side tends to radiate the rear wave. This type of diaphragm can be made to generate a close to ideal spherical wave over a wide bandwidth when connected to an appropriate tapering duct (see for example [13]).
- The required entrance area of the metamaterial absorber is reduced by the tapered duct and this reduces the thickness of the metamaterial absorber fairly substantially.
- The tapered duct occupies less space than a straight duct and makes it easier to accommodate this into a loudspeaker design where other parts are competing for space, especially in a coaxial driver configuration.

Figure 14b shows the final implementation of the metamaterial absorber into the high-frequency unit. The length of the tube is 60 mm, sufficiently short to have the first resonance frequency around $4f_c$. Figure 15 represents the absorption spectrum of the metamaterial absorber when the conical horn is filled with 20 kg/m$^3$ polyester fibre to smooth out the response [14]. The role of the fibrous material is as an absorption valley-filler and to fine tune the knee of the absorption spectrum. The absorption reaches the astonishing value of 99% from 620 Hz with the 11 mm thick metamaterial whereas the 120 mm long exponential horn depicted in Figure 14a struggles to exceed 80%. The ripples are induced by the truncation of the horn. Adding more wadding in the exponential horn helps smoothing out the response but it is not sufficient and the only way to achieve the same performance as the metamaterial is to reduce the cut-off frequency and increase the length of the exponential horn to half a meter.

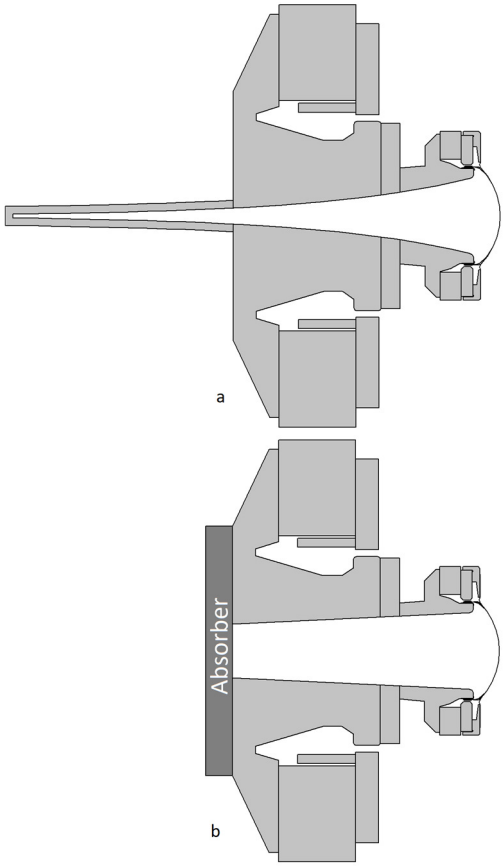


Figure 14 – Cross-section of a coaxial driver where the back of the tweeter dome is either connected to an exponential horn (a) or to the radial metamaterial absorber through an optimised conical duct (b).

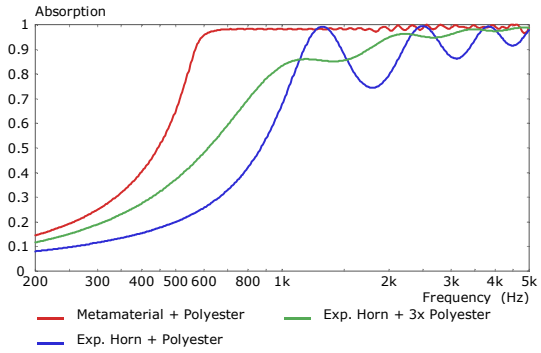


Figure 15 – Absorption at the entrance of the conical duct connected to the metamaterial absorber compared to an exponential horn of the same entrance size. Both are filled with polyester fibres.

## Conclusion

The implementation of an extremely innovative metamaterial absorber in a loudspeaker driver has been presented. The causal-optimal broadband absorber relies on a predesigned multi-resonator unit optimally packed in a very thin disk located at the back of the drive unit. A key aspect of the successful implementation is the optimal coupling between the loudspeaker diaphragm and the metastructure through a specific conical duct. The performance far exceeds the limits of conventional sound-absorbing structures such as reversed horns, achieving almost a near-perfect absorption spectrum starting at 620 Hz with a physical thickness of 11 mm only whereas an exponential horn needs half a meter to reach equal performance.

## Acknowledgments

The authors would like to thank Acoustic Metamaterials Group for providing the design and geometry of the metamaterial structures; and Andy Whitewood for his work on the mechanical design and the impedance tube fabrication.

## References

[1] L. E. Kinsler, Fundamentals of Acoustics, Wiley, 1982.

[2] R. H. Small, "Closed-Box Loudspeaker Systems-Part 1: Analysis," *J. Audio Eng. Soc.,* vol. 20, no. 10, pp. 798-808, Dec. 1972.

[3] J. Allard and N. Atalla, Propagation of Sound in Porous Media: Modelling Sound Absorbing Materials, Wiley & Sons, 2009.

[4] F. E. Terman, "Sound Absorbing Apparatus". Patent US2293181A, 17 July 1940.

[5] L. Chisari, M. Di Cola and P. Martignon, "Acoustic Metamaterials in Loudspeaker Systems Design," *147th Audio Eng. Soc. Convention* , 2019.

[6] M. Yang and P. Sheng, "Sound Absorption Structures: From Porous Media to Acoustic Metamaterials," *Annu. Rev. Mater. Res.,* vol. 47, pp. 83-114, July 2017.

[7] M. Yang, S. Chen, C. Fu and P. Sheng, "Optimal sound-absorbing structures," *Mater. Horiz.,* vol. 4, pp. 673-680, 2017.

[8] R. M. Fano, "Theoretical limitations on the broadband matching of arbitrary impedances," *J. Franklin Inst.,* vol. 249, no. 1, pp. 57-83, 1950.

[9] K. N. Rozanov, "Ultimate thickness to bandwidth ratio of radar absorbers," *IEEE Trans. Antennas and Propag.,* vol. 48, no. 8, pp. 1230-1234, 2000.

[10] C. R. Hanna and J. Slepian, "The Function and Design of Horns for Loudspeakers," vol. 43, pp. 393-411, Feb. 1924.

[11] ISO10534-2, *Acoustics - Determination of sound absorption coefficient and impedance in impedance tubes - Part 2: Transfer-function method,* 1998.

[12] B. Kolbrek and T. Dunker, High-Quality Horn Loudspeaker Systems, Kolbrek Elektroakustikk, 2019.

[13] M. Dodd, "Loudspeaker". Patent US8094854B2, 2005.

[14] M. Garai and F. Pompoli, "A simple empirical model of polyester fibre materials for acoustical applications," *Applied Acousctics,* vol. 66, no. 12, pp. 1383-1398 , Dec. 2005.